Engineering Educators Bringing the World Together
2025 ASEE Annual Conference & Exposition
Palais des congrès de Montréal, Montréal, QC • June 22–25, 2025 ASEE
Paper ID #48848

BYOE: Building Robust VR Learning Environments: Best Methods to Visualize divergence-free Vector Fields

Alex Shaffer, University of Illinois at Urbana - Champaign
Prof. Raluca Ilie, University of Illinois Urbana-Champaign

Prof. Ilie is an Assistant Professor in the Department of Electrical and Computer Engineering at the University of Illinois at Urbana-Champaign. Her primary research is the development and application of high-performance, first principles computational models to describe and predict the conditions in near-Earth space leading to geomagnetic storms. Prof. Ilie's research focus is on developing new approaches to study the dynamics of plasmas and electromagnetic fields in the geospace environment, and to advance the predictive capabilities of the complex dynamics occurring in the solar wind-magnetosphere-ionosphere system. She combines both theoretical and observational work to develop predictive tools that form the basis of operational warning systems and hazard mitigation.

Prof. Ilie has been recognized as an emerging leader in education by her selection to the Strategic Instructional Innovations Program, to develop Virtual reality (VR) simulations and learning environments to support student learning for electrical engineering courses.

Prof. Ilie earned her Ph.D in Space and Planetary Physics from the University of Michigan and has been an NSF Postdoctoral Fellow at Los Alamos National Laboratory. As part of the Center for the Space Environment Modeling at University of Michigan, she was a core member of the software developing team for the Space Weather Modeling Framework. She is a recent awardee of the NSF CAREER, NASA Heliophysics Early Career Investigator and Air Force Young Investigator Program awards.

BYOE: Building Robust VR Learning Environments: Best Methods to Visualize divergence-free Vector Fields

Introduction

The theory of electromagnetism (E&M), encapsulated in the four Maxwell's equations, is at the core of Electrical Engineering. When James Clerk Maxwell first published "A Dynamical Theory of the Electromagnetic Field" in 1865, physicists found it difficult to grasp because the theoretical framework seemed complicated. Mathematicians also found Maxwell's work hard to understand because the equations were described in physical terms. Students nowadays still encounter difficulty grasping the principles pertaining to electromagnetism due to a lack of intuitive familiarity with the phenomena. However, developing this intuition is limited by the 2D nature of traditional display technologies, which cannot truly convey the three-dimensional (3D) nature of E&M concepts. Advances in Virtual Reality (VR) and Augmented Reality (AR) display devices hold great promise in helping students build a physical intuition regarding electromagnetism.

Several studies have explored the use of AR for instruction, particularly to teach E&M concepts. For instance, it has been shown that AR provided students with a better understanding of Fleming's rule than traditional 2D techniques [1]. Existing work demonstrates the ability to render real-time magnetic field lines of magnetic dipoles in a 2D plane using AR [2]. This was expanded on through the development of a 3D AR visualization tool for magnetic dipoles, tracing magnetic field lines with a modified version of the Euler forward algorithm described below [3]. While these studies explored the use of AR to help visualize electromagnetic concepts, the work presented in this study employs Virtual Reality, as it allows for control over the entirety of the learning environment and has more accessible and available hardware than augmented reality.

One of the four Maxwell's equations, Ampere's Law, states that distributions of electrical currents seed magnetic fields. Understanding the abstractions built in this law of physics requires the ability to visualize these vector fields and their interactions in a 3D environment. Numerical methods exist for accurately tracing field lines in divergence-free fields [4–6], but are often prohibitively computationally expensive to perform well in real-time. This paper discusses the suitability of three numerical methods for interactive visualization of divergence-free vector fields in VR, as well as approximation techniques that may be used in cases where these numerical methods perform poorly.

Methodology

The development of a robust visualization technique to illustrate the concepts pertaining to the generation of magnetic fields is the primary goal of this study, as the magnetic field is the only field that appears in Ampere's law (shown in Equation 1) in the absence of displacement currents $\partial_t \mathbf{E}$, such that static current densities **(J)** are the only sources of magnetic field. Note that μ_0 represents the free space magnetic permeability.

$$\nabla \times \mathbf{B} = \mu_0(\mathbf{J} + \epsilon_0 \partial_t \mathbf{E}) \tag{1}$$

Furthermore, the magnetic field belongs to a class of vector fields that are divergence-free, as described by one of the four Maxwell's equations, which states that magnetic monopoles do not exist in nature. Consequently, every north magnetic pole is always accompanied by a south magnetic pole, as shown in Equation 2.

$$\nabla \cdot \mathbf{B} = 0 \tag{2}$$

In general, the concept of field lines is a common and effective method of visualizing vector fields, and it is particularly common in the literature for visualizing electric and magnetic fields. Other techniques for visualizing vector fields are glyph plots and line integral convolutions. While glyph plots and line integral convolutions [7] are effective methods for visualizing vector fields in 2D, in 3D the glyph plots frequently become too cluttered, and the line integral convolution does not translate well to a three-dimensional domain. Field line visualization adapts well to 3D as the curves that describe the field line gain another degree of freedom.

For applications in virtual reality, the visualization method must be computationally efficient so it can produce a visualization in real-time. This is particularly important for interactive educational experiences, in which we seek to leverage the advantages of active learning. With the correct choice of numerical integration method, field line visualizations are efficient enough to run in real-time. It is necessary to use numerical integrators because a vector field in 3D can be thought of as three first-order ordinary differential equations. The Euclidean x, y, and z components of the vector field are the x, y, and z derivatives, respectively, of the differential equations. The solutions of these differential equations describe the set of points that make up a field line with an initial condition of a starting point. Three integrators are tested in this study: the Euler forward, Heun's method, and the fourth-order Runge-Kutta method (RK4), which have been adapted from the algorithms described in *Numerical solution of ordinary differential equations* [8].

These methods may be applied to systems such as assortments of infinitely long current-carrying wires, as the solution for the magnetic field generated by one such configuration is relatively simple, as shown in Equation 3 from [9]:

$$\mathbf{B} = \frac{\mu_0 I}{2\pi s}\hat{\phi} \tag{3}$$

where s represents the perpendicular distance from the wire, and $\hat{\phi}$ is the azimuthal basis vector, and I is the current magnitude. When multiple sources (current-carrying wires) are present, the resulting magnetic field is the sum of all fields sourced by each individual wire, according to the principle of superposition. Therefore, it is possible to visualize the magnetic field associated with a system containing an arbitrary number of infinite current-carrying wires in a VR environment. The user may interactively manipulate the position of these wires, and the visualization will update the solution for the magnetic field in real-time according to the updated position of each wire. While the wires appear to have a finite length in the visualization, their associated magnetic fields are modeled using the infinite wire solution (see Equation 3).

Below, we briefly describe the procedure employed by each of the methods tested. For a magnetic field $\mathbf{B}(\mathbf{r})$, a field line is approximated by a polygonal chain, an ordered set of points with linear connections. From that, the field line length $s_B = (N-1)\Delta s$, where N is the number of points along the field line, and Δs represents the step size.

Euler Forward

i. Begin at an arbitrary starting position $\mathbf{r}_0$ and with a magnetic field $\mathbf{B}(\mathbf{r})$. The associated field line is determined from a maximum number of steps N and a step size Δs.

ii. $\mathbf{r}_{i+1} = \mathbf{r}_i + \Delta s \mathbf{B}(\mathbf{r}_i)$.

iii. The set of all points r_i, with $i \in [0, N-1]$ make up a discrete approximation to a field line of $\mathbf{B}(\mathbf{r})$.

Heun's Method

i. Begin at an arbitrary starting position $\mathbf{r}_0$ and with a magnetic field $\mathbf{B}(\mathbf{r})$. The associated field line is determined from a maximum number of steps N and a step size Δs.

ii. $\mathbf{r}_{i+1} = \mathbf{r}_i + \frac{\Delta s}{2}(\mathbf{B}(\mathbf{r}_i) + \mathbf{B}(\tilde{r}_i))$, where $\tilde{r}_i = \mathbf{r}_i + \Delta s \mathbf{B}(\mathbf{r}_i)$

iii. The set of all points r_i, with $i \in [0, N-1]$ make up a discrete approximation to a field line of $\mathbf{B}(\mathbf{r})$.

RK4

i. Begin at an arbitrary starting position $\mathbf{r}_0$ and with a magnetic field $\mathbf{B}(\mathbf{r})$. The associated field line is determined from a maximum number of steps N and a step size Δs.

ii. $\mathbf{r}_{i+1} = \mathbf{r}_i + \frac{\Delta s}{6}(k_1 + 2k_2 + 2k_3 + k_4)$, where $k_1 = \mathbf{B}(\mathbf{r}_i)$, $k_2 = \mathbf{B}(\mathbf{r}_i + \Delta s \frac{k_1}{2})$, $k_3 = \mathbf{B}(\mathbf{r}_i + \Delta s \frac{k_2}{2})$, and $k_4 = \mathbf{B}(\mathbf{r}_i + \Delta s k_3)$

iii. The set of all points r_i, with $i \in [0, N-1]$ make up a discrete approximation to a field line of $\mathbf{B}(\mathbf{r})$.

In order to trace magnetic field lines, numerical integration techniques are coupled with a set of termination conditions. Since magnetic fields are divergence-free in nature, magnetic field lines must close on themselves. This property is challenging to reproduce numerically; therefore, in order to efficiently trace these magnetic field lines, the numerical integration method is subjected to the following termination conditions: (i) if the integration reaches a predetermined maximum number of steps, and (ii) if the field line reconnects with itself at its starting point. The latter is

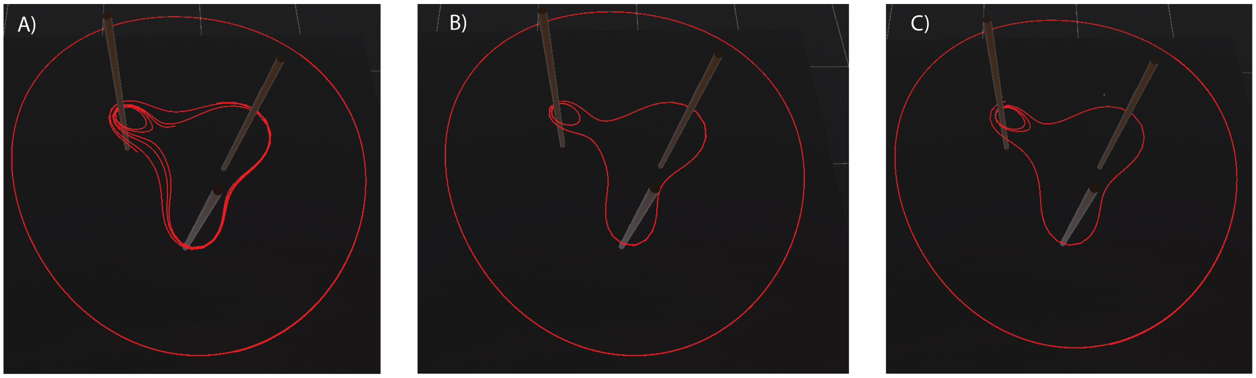

Figure 1: A system of three infinite wires generating a magnetic field. Three field lines are traced using A) Euler Forward, B) Heun's method, and C) RK4

ensured by checking whether the first and last points on the field line are within a very small distance and if the tangent vectors at the field line's starting and end points are nearly parallel.

To compare the numerical integration methods employed here, the local and global truncation errors are evaluated for each method. The local truncation error is the error associated with the one step of the numerical integrator as compared with the analytical solution. The global truncation error is the accumulated local truncation error over all of the steps of the numerical integrator. For Euler's method, the local error is proportional to the square of the step size Δs, that is, $\mathcal{O}(\Delta s^2)$ [8]. Heun's method has a local error of $\mathcal{O}(\Delta s^3)$ while RK4 has a local truncation error of $\mathcal{O}(\Delta s^5)$. It can be shown that if the local truncation error is $\mathcal{O}(\Delta s^n)$ then the global truncation error is $\mathcal{O}(\Delta s^{n-1})$, one order lower than the local error [8]. This means that for a small step Δs, Heun's method has a smaller local and global truncation error than Euler's method, while RK4 yields yet smaller errors. Therefore, it is expected that RK4 would produce more accurate field lines. However, numerical accuracy does not necessarily always correspond to visually identifiable properties of field lines, such as reconnection. Figure 1 illustrates this point, as Heun's method more frequently met the reconnection termination condition when compared with either Euler forward or RK4.

Each of these numerical integration techniques comes at a different computational cost. A meaningful measure of the relative cost of each of these methods is the number of times it needs to evaluate the magnetic field at a given point in each iteration step. While other operations are performed in each method, determining the value of the magnetic field at a given point requires a large number of floating point operations (FLOPS). The Euler forward method requires one of these function calls in each step, Heun's method requires two calls, while RK4 requires four function calls. This makes RK4 the most computationally expensive method and Euler forward the least computationally expensive method.

Numerical integrators work and perform well for cases such as a system of infinite current-carrying wires. However, in some cases, it can be challenging to create field line visualizations using these aforementioned methods. For instance, the magnetic field vector needs to be calculable at every point in the domain space, and stability conditions need to be met for

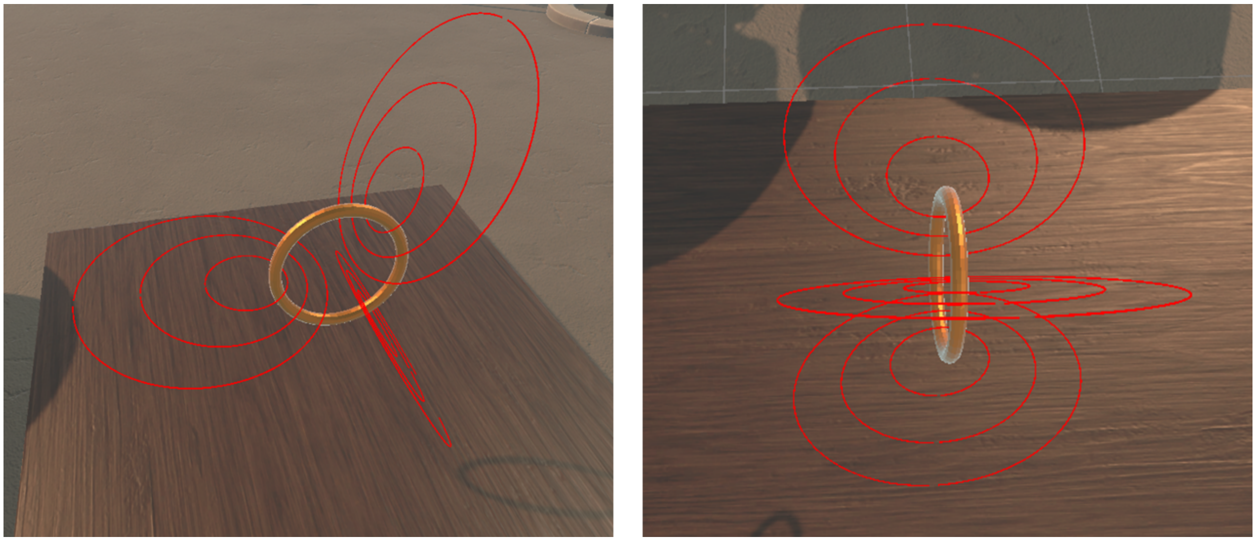

Figure 2: Magnetic field lines generated from a current-carrying loop approximated with ellipses.

large enough step sizes for the algorithms to perform in real-time efficiently. An example illustrating a scenario where such difficulties can arise is provided by the current-carrying wire loop depicted in Figure 2. In this case, the calculation of the magnetic field and the subsequent visualization of magnetic field lines proves to be challenging, as it requires computing elliptic integrals of the first and second kind [10], a computationally expensive task, especially since it must be performed frequently. Therefore, for a system in which the current loop's position in space changes, real-time computation of the magnetic field using either Euler forward, Heun's method, or RK4 is unfeasible, as these methods have demonstrated poor performance. In such cases, it may be necessary to resort to alternative methods, such as a precomputed and approximated set of field lines.

Summary and discussion

For the purpose of educational visualizations, the instructional value takes precedence over the display of exceedingly accurate numerical solutions. It is, however, essential to convey the core concepts with clarity. Therefore, certain approximations can significantly enhance the performance and interactivity without compromising the fundamental concepts. For example, in the case of a current-carrying loop wire, approximations can be made to simplify the exact shape of the field lines while preserving its essential characteristics. They may be approximated as nested ellipses looping around the wire, as shown in Figure 2. This approach maintains the intrinsic rotational symmetry of a current-carrying loop's associated magnetic field while ensuring that the shape and centers of the field lines remain visually accurate. This simple approximation avoids the computationally intense process of numerical integration and enhances real-time interactivity.

For the purpose of visualizing magnetic field lines in an interactive real-time VR environment, we found Heun's method to be the best performing out of the three numerical integration techniques tested. Heun's method provided a combination of accuracy and low computational cost that made it best suited for producing visualizations of magnetic field lines with reasonable fidelity. Typically, VR frameworks must display at least 120 frames per second (FPS) to eliminate motion sickness [11]. Heun's method consistently maintained a frame rate above 120 FPS, while RK4 occasionally dropped below this threshold. Although RK4 is associated with a lower truncation error, it was found to be computationally demanding and less suitable to perform in real-time in a virtual reality environment.

The methods for visualizing magnetic fields used in this study can be applied and ported to any other divergence-free vector fields. For example, incompressible fluids exhibit a divergence-free flow velocity [12], similar to the behavior of magnetic fields. Therefore, visualizing streamlines through these fluids, the equivalent of field lines for magnetic fields, may be approached in a similar manner. This makes these numerical methods relevant to a broader range of educational visualizations, particularly in physics and engineering fields. Beyond electromagnetism, similar approaches can be applied to fluid dynamics, aerodynamics, and plasma physics, where understanding vector fields is essential. By leveraging these techniques, educators can create interactive simulations that enhance students' conceptual understanding of complex phenomena, such as airflow over surfaces, heat transfer in fluids, and electric and magnetic field interactions.

Acknowledgments

Work at the University of Illinois at Urbana-Champaign was performed with financial support from the NSF CAREER award 1945573.

References

[1] Harun, N. Tuli, and A. Mantri, "Experience Fleming's rule in electromagnetism using augmented reality: Analyzing impact on students learning," *Procedia Computer Science*, vol. 172, pp. 660–668, 2020, 9th World Engineering Education Forum (WEEF 2019) Proceedings : Disruptive Engineering Education for Sustainable Development. [Online]. Available: https://www.sciencedirect.com/science/article/pii/S1877050920314150

[2] S. Matsutomo, T. Miyauchi, S. Noguchi, and H. Yamashita, "Real-time visualization system of magnetic field utilizing augmented reality technology for education," *IEEE Transactions on Magnetics*, vol. 48, no. 2, pp. 531–534, 2012.

[3] S. Matsutomo, T. Manabe, V. Cingoski, and S. Noguchi, "A computer aided education system based on augmented reality by immersion to 3-d magnetic field," *IEEE Transactions on Magnetics*, vol. 53, no. 6, pp. 1–4, 2017.

[4] M. Zhang and X. Feng, "A comparative study of divergence cleaning methods of magnetic field in the solar coronal numerical simulation," *Frontiers in Astronomy and Space Sciences*, vol. 3, 2016. [Online]. Available: https://www.frontiersin.org/journals/astronomy-and-space-sciences/articles/10.3389/fspas.2016.00006

[5] K. G. Powell, P. L. Roe, and J. Quirk, "Adaptive-mesh algorithms for computational fluid dynamics," in *Algorithmic Trends in Computational Fluid Dynamics*, M. Y. Hussaini, A. Kumar, and M. D. Salas, Eds. New York, NY: Springer New York, 1993, pp. 303–337.

[6] K. G. Powell, P. L. Roe, T. J. Linde, T. I. Gombosi, and D. L. De Zeeuw, “A solution-adaptive upwind scheme for ideal magnetohydrodynamics,” *Journal of Computational Physics*, vol. 154, no. 2, pp. 284–309, 1999. [Online]. Available: https://www.sciencedirect.com/science/article/pii/S002199919996299X

[7] B. Cabral and L. C. Leedom, “Imaging vector fields using line integral convolution,” in *Proceedings of the 20th Annual Conference on Computer Graphics and Interactive Techniques, SIGGRAPH 1993, Anaheim, CA, USA, August 2-6, 1993*, M. C. Whitton, Ed. ACM, 1993, pp. 263–270. [Online]. Available: https://doi.org/10.1145/166117.166151

[8] K. E. Atkinson, W. Han, and D. Stewart, *Numerical solution of ordinary differential equations*, ser. Pure and applied mathematics. Hoboken, N.J: Wiley, 2009.

[9] D. J. Griffiths, *Introduction to Electrodynamics*, 5th ed. Cambridge University Press, 2023.

[10] M. Ortner, P. Leitner, and F. Slanovc, “Numerically stable and computationally efficient expression for the magnetic field of a current loop,” *Magnetism*, vol. 3, no. 1, pp. 11–31, 2023. [Online]. Available: https://www.mdpi.com/2673-8724/3/1/2

[11] J. Wang, R. Shi, W. Zheng, W. Xie, D. Kao, and H.-N. Liang, “Effect of frame rate on user experience, performance, and simulator sickness in virtual reality,” *IEEE Transactions on Visualization and Computer Graphics*, vol. 29, no. 5, pp. 2478–2488, 2023.

[12] V. John *et al.*, *Finite element methods for incompressible flow problems*. Springer, 2016, vol. 51.